Attosecond pulse generation, measurement and applications on solids

Reinhard Kienberger

Fakultät für Physik, E11, Technische Universität München, James Franck Straße, 85748 Garching,

Max Planck Institut für Quantenoptik, Hans Kopfermann Str. 1, 85748 Garching.

Attosecond XUV pulses (80 *as*, 1 *as* = 10^{-18} *s* [1, 2]) together with phase-stabilized few-cycle (few-femtosecond) laser pulses [3] used for their generation have enabled the development of a technique for attosecond sampling of electrons ejected from atoms or molecules [4, 5]. After the generation of attosecond pulses on a daily base and their characterization at high precision has been made possible, the dynamics of the photoionization process on solids has been studied [6]. Not only that attosecond metrology now enables clocking on surface dynamics, but also the individual behaviour of electrons of different type (core electrons vs. conduction band electrons) can be resolved. Here, we measured a time delay of about 100 *as* on the emission of the aforemention two types of electrons. The information gained in these experiments may have influence on the development of many modern technologies including semiconductor and molecular electronics, optoelectronics, information processing, electrochemical reactions, etc..

Efforts to access ever shorter time scales are motivated by the endeavour to explore the microcosm in ever smaller dimensions. The measurement of ever shorter intervals of time and tracing dynamics on the atomic time scale relies on the reproducible generation of ever briefer events and on probing techniques of corresponding resolution [7]. Reproducible generation and accurate measurement of isolated sub-femtosecond extreme ultraviolet (XUV) pulses – along with novel measurement techniques – now open to way to tracing electronic dynamics deep in

Nonlinear Optics and Applications V, edited by Mario Bertolotti, Proc. of SPIE Vol. 8071
80710G · © 2011 SPIE · CCC code: 0277-786X/11/$18 · doi: 10.1117/12.887378

the interior of atoms, molecules and solids directly in the time-domain with a resolution well within the classical Bohr orbit time in the inner orbit of the hydrogen atom (150 as).

Intense laser pulses consisting of a few, precisely-controlled oscillations of the electric field [3] constitute the key to both the generation of isolated attosecond pulses and time-resolved measurements on an attosecond time scale. The electric field of linearly-polarized femtosecond laser pulses, if sufficiently strong, induces – in a highly nonlinear interaction – gigantic dipole oscillations by pulling an electron out of the atom and smashing it back towards its core half a cycle later. The oscillations are not sinusoidal but contain very high frequency components extending into the extreme ultraviolet and soft-X-ray regime [8]. In a laser field containing many oscillation cycles, the oscillations are repeated quasi-periodically, resulting in the emission of a series of high-energy bursts of sub-femtosecond duration and high-order harmonics of the laser radiation in the spectral domain. For a few-cycle laser driver only a few dipole oscillations, different in amplitude occur. The oscillation with the highest amplitude has been predicted to produce a single burst in the spectral range of the highest emitted photon energies [3]. With waveform-controlled few-cycle light, the few giant atomic dipole oscillations induced can be precisely controlled and reproduced from one laser shot to the next. This is expected to result in an XUV burst with parameters well reproduced from one shot to the next. State of the art are single, isolated 80-as-pulses in the range of 100 eV photon energy [9].

The synchronism of the XUV burst to the field oscillations of the generating laser pulse offers the potential for using the XUV burst *in combination with* the oscillating laser field for attosecond spectroscopy. This is essential because these laser-produced XUV bursts are too weak to be used for *both* triggering *and* probing

electronic dynamics (XUV-pump/XUV-probe spectroscopy). Instead the oscillating laser field, which changes its strength from zero to maximum within some 600 attoseconds in a 750-nm laser wave, can take over the role of the probing XUV pulse. In the following we shall see how the hyperfast electric field oscillations of the few-cycle visible laser pulse that previously produced the sub-femtosecond XUV burst can be employed for taking "tomographic images" of the time-momentum distribution of electrons ejected from atoms following an impulsive excitation by the synchronized XUV burst. Probing photo- or Auger–electrons yields insight into excitation and subsequent relaxation processes, respectively. The transients can be triggered by an isolated attosecond electron or photon burst synchronized to the probing light field oscillations. The technique draws on the basic operation principle of a streak camera [10-14] where a light pulse generates an electron bunch having exactly the same temporal structure. The deflection of the electrons in an electric field allows the reconstruction of the duration of the electron bunch. By measuring the temporal evolution of emission intensity *and* momentum distribution of positive-energy electrons, the atomic transient recorder (ATR) provides direct temporal insight into the rearrangement of the electronic shell of excited atoms on a sub-femtosecond scale [5].

Inspired by the physics of the first sub-femtosecond experiment [1], the basic concept for ATR metrology was put forward by Corkum and coworkers [13] and analyzed with a quantum theory by Brabec and coworkers [14]. Consider electron emission from atoms exposed to a sub-fs XUV burst in the presence of an intense, linearly-polarized, few-cycle laser field $E_L(t) = E_0(t)cos(\omega_L t + \varphi)$. The momentum of the freed electrons is changed by $\Delta p = eA_L(t)$ along the laser field vector. Here $A_L(t_r) = \int_{t_r}^{\infty} E_L(t)dt$ is the vector potential of the laser field, e and m stand for

the charge and rest mass of the electron, respectively, and t_r is the release time of the electron. This momentum transfer (arrows in Fig. 1b) maps the temporal emission profile into a similar distribution of final momenta $p_f = p_i + \Delta p$ within a time window of $T_0/2 = \pi/\omega_L$, if the electrons' initial momentum p_i is constant in time and their emission terminates within $T_0/2$. Under these conditions the temporal evolution of the electron emission (profiles on the horizontal axis in Fig. 1b) can be unambiguously

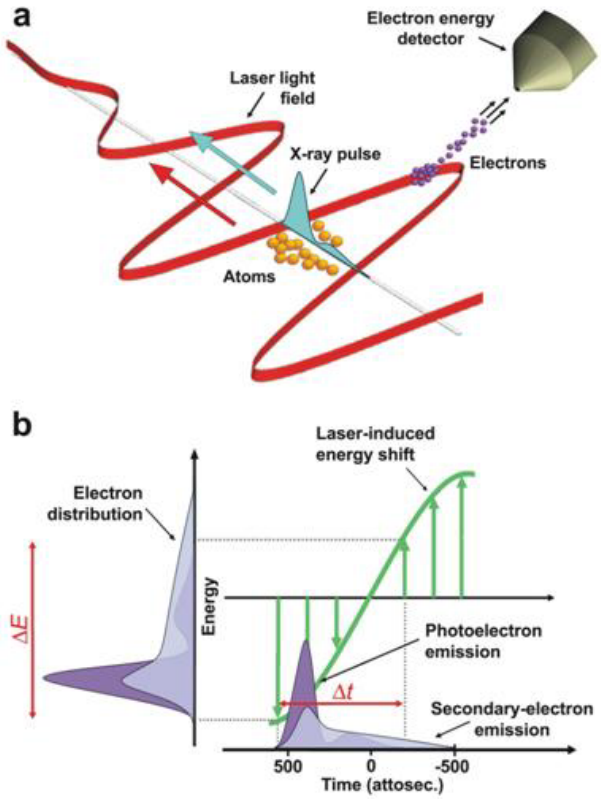

Figure 1 Light-field-controlled streak camera. The attosecond XUV flash excites the atoms, which then emit electrons. The electrons ejected in the direction of the electric field of the laser light pulse simultaneously beamed in are detected. They undergo - depending on the time of their emission within half the oscillation period of the laser light - a change of velocity: in the case illustrated the electrons emitted first are decelerated, while those released on termination of the XUV flash are accelerated. In this manner the successively emitted electrons are detected separately, but not spatially on a screen but alongside one another *on the energy scale*. The width ΔE and shape of the measured energy distribution (vertical axis in Fig. 1 b) of the electrons reflect the duration and evolution of the electron emission, just as their spatial distribution in conventional streak imaging. In this case, however, "deflection" occurs within half a light period, which opens the way to measurement in the attosecond region (from [7]).

retrieved from a single "streaked" momentum distribution (profiles on the vertical axis in Fig. 1b). However, any sweep of the electrons' initial momentum revokes the unique correspondence between the electron's final momentum and release time, preventing the retrieval of accurate temporal information from single streak records.

In general, the initial momentum spectrum of electrons detached from atoms by an impulsive excitation is varying in time during emission resulting in a time-momentum distribution $n_e(p, t)$ of electron emission rate. The final electron momentum spectrum, $\sigma(p) = \int_{-\infty}^{\infty} n_e(p,t)dt$, can be viewed as the projection of the time-dependent momentum distribution on the momentum space along lines of constant p. In the classical description of the freed electrons' motion in the strong laser field, the final spectra obtained in the presence of a strong laser field are generalized projections along lines where $p_f = p_i + eA_L(t)$ is constant. By delaying the laser field with respect to the the excitation that triggers electron emission, we obtain a set of tomographic records (briefly: streaked spectra),

$$\sigma_A(p) = \int_{-\infty}^{\infty} n_e(p - eA_L(t), t)dt, \qquad (1)$$

from which, with a suitable set of $A_L(t - \Delta t_n)$, the complete distribution $n_e(p, t)$ can be reconstructed. The method is closely related to frequency-resolved optical gating [15,16] with the oscillating field as a gate. In the simplest cases two streaked spectra (in addition to the field-free spectrum) may be sufficient. In the absence of a nonlinear momentum sweep the streak records obtained near the zero transitions of $A_L(t)$ with opposite slopes together with the field-free spectrum allow determination of all relevant characteristics: the temporal profile, duration and monentum chirp of emission.

With these tools – reproducible attosecond pulses to trigger electronic processes and a suitable measurement technique, the atomic transient recorder (ATR) - at hand, dynamics on solid surfaces have been studied [6,17]. In the case of multiple, distinct emission lines in the photoelectron spectrum like in solids, the ATR can be used to compare the characteristics of the photoelectrons originating from the different states. For example, the photoelectron spectrum of a (110)-oriented tungsten surface obtained with attosecond XUV pulses (Fig. 2) shows two distinct peaks originating from 5d/6sp valence band electrons and 4*f* /5p core levels.

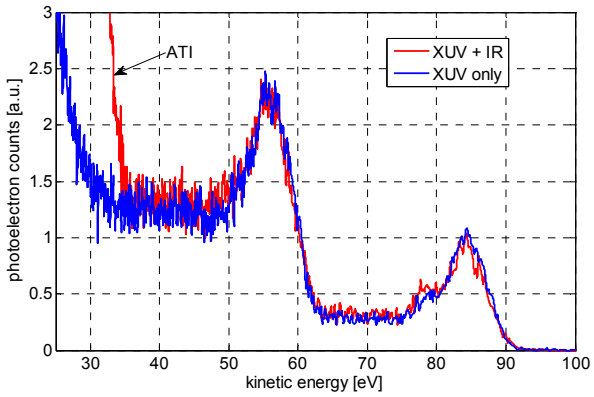

Fig. 2: Raw photoelectron spectra of tungsten (110) measured with (red curve) and without (blue curve) the presence of the probe NIR streaking field using XUV photons of ~91 eV. The spectra show two distinct peaks originating from 5d/6sp valence electrons and 4*f*/5p core levels at ~83 and ~56 eV, respectively. In the presence of the NIR probe field, there is an intense photoelectron signal below 35 eV induced by above threshold ionization (ATI). Each spectrum was obtained by integration over 60,000 laser pulses (from [17]).

By employing the ATR, the relative timing of the photoelectrons emerging through the surface can be determined. As is illustrated in Figure 3, photoelectrons traversing the surface at different instants of time are subject to different phases of the streaking field. It is possible to extract an effective emergence time of the electrons using the waveform controlled streaking field even though it penetrates the bulk due to the optical index of refraction, thereby modifying sub-surface transport and spectral shape

to some extent. As a result, the effective delay in photoemission can be reconstructed from the spectrograms (Figure 4a).

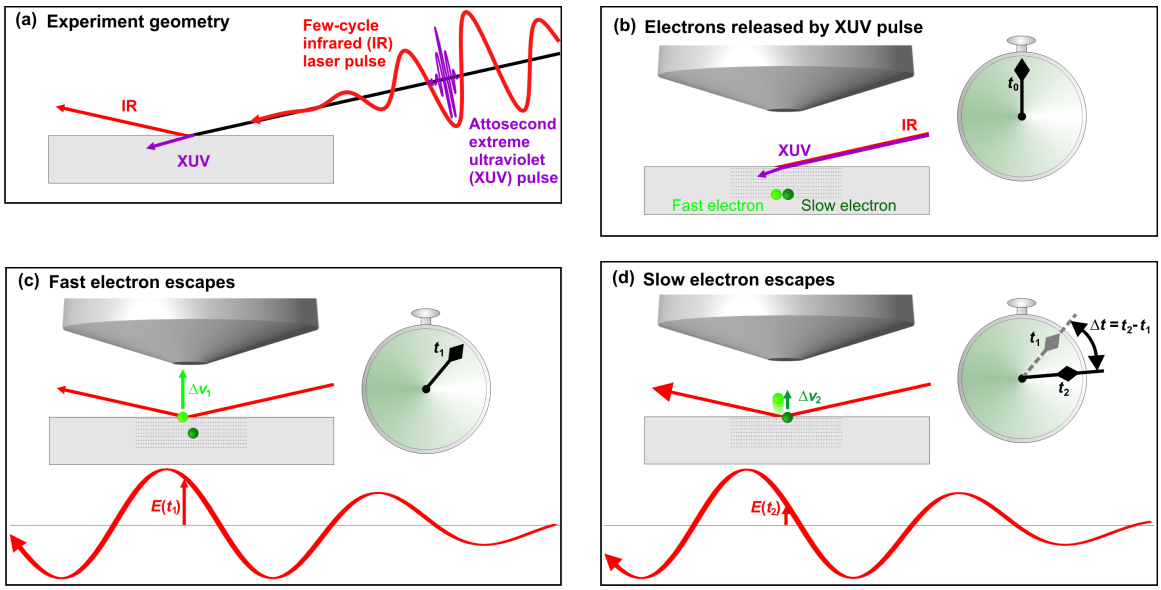

Fig. 3: Attosecond spectroscopy on solids: Electrons arriving at the surface at different instants of time are subject to different phases of the streaking field outside the metal (in this fig., we neglect the streaking field inside the solid which due to the metal's optical properties is weak) In panel (a) an isolated attosecond XUV pulse and a delayed few-cycle waveform controlled streaking field are incident on a solid surface. In panel (b), at time t_0, the XUV pulse is absorbed in the solid and two types of photoelectrons are born, for simplicity one photoelectron is called "slow" the other "fast". In panel (c), at time t_1, the fast electron has propagated to the surface and is now subject to the strong streaking field, which modulates its outgoing kinetic energy depending on the instant of release. In panel (d) at time t_2, the slow electron has reached the surface and feels the strong streaking field at the vacuum side; since it has emerged at a different time, the modulation of its kinetic energy will vary depending on the precise delay in emission. By evaluation of the full streaking spectrograms, collected as a function of relative delay between the attosecond XUV pulse and the streaking field, the delay in photoemission can be determined. Compared to streaking experiments at isolated particles, detailed models of electron localization, and electron and photon transport and interaction are necessary for the evaluation of such spectrograms (from [17]).

Both spectrograms show the change in electron energy corresponding to the evolution of the electric field of the NIR streaking pulse. Figure 4b shows a centre-of-mass (COM) analysis of the spectrograms. For this analysis, the time-dependent COM of both emission lines were calculated in a global fit by:

$$COM_{CB}(t) = a_1 \, \mathrm{e}^{-4\ln(2)\frac{(t-t_0)^2}{FWHM^2}} \sin(\omega t + \phi_0) + offset_{CB},$$

$$COM_{4f}(t) = a_2 \, \mathrm{e}^{-4\ln(2)\frac{(t-t_0-\Delta t)^2}{FWHM^2}} \sin(\omega t + \phi_0 - \omega\Delta t) + offset_{4f},$$

where a_1, a_2, $offset_{CB}$ and $offset_{4f}$ denote the streaking amplitudes and the time-independent positions of the emission lines, respectively. t_0 and $FWHM$ denote center and full width at half maximum of the Gaussian-shaped envelope of the streaking field, and ϕ_0 gives its carrier envelope phase. The parameter Δt accounts for a temporal shift between the spectrograms of both emission lines. The fit results are shown as solid lines in Figure 4b and a temporal shift in the streaking of 85 ± 45 as corresponding to the same delay in emission of the photoelectrons from the tungsten surface is extracted. This result is in good agreement with the initial study, where valence electrons were found to be emitted approximately 100 attoseconds earlier than their tightly-bound core-state counterparts [6].

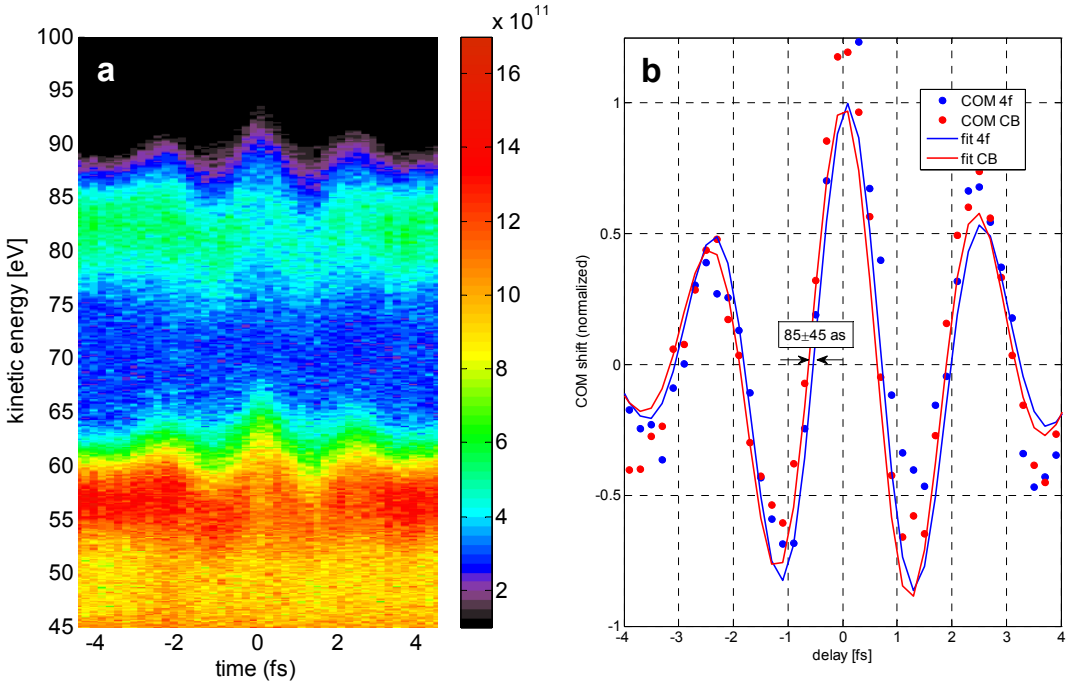

Fig. 4: a) Raw ATR spectrogram of a tungsten (110) surface. Photoelectron intensities are given in arbitrary units. b) Center-of-mass (COM) analysis of the spectrogram. The COM of both emission lines as measured are given as dots, a global fit to both COM traces is shown in solid lines (from [16]).

These results demonstrate the technical capability of measuring photon induced electron release, electron transport through the topmost atomic layers of a solid sample, and emission into the vacuum in real time, with attosecond temporal resolution. Explaining the state dependent differences of these emission dynamics seen in the streaking experiment is unfortunately a much more challenging task than its equivalent for isolated particles [5].

The fact that different theoretical approaches based on rather different assumptions yield contradicting explanations for the experimentally observed electron emission dynamics from a metal surface [5,18-20], yet numerical values for the expected delay which all are within the experimental scatter, clearly indicates that the streaking

process at solid surfaces is not well understood. Many processes and properties, such as primary photoemission, screening by itinerant electrons, transport including elastic and inelastic scattering in the bulk and across the solid/vacuum interface, the influence of the streaking field inside the material, and the localization of the individual electronic states contribute to the effect. The next set of experiments must help to solve this puzzle. A homogeneous sample like tungsten with its overlapping localized (5d) and delocalized (6sp) valence electrons, and core levels of different symmetry (5p, 4f) that are energetically not resolvable under the conditions of an attosecond photoemission experiment, may be too complex for this purpose. Well-tailored samples, and experiments performed on these samples with different photon energies are required to disentangle the individual contributions of the above processes to the overall delay observed in the experiment. Such samples could be thin crystalline layers heteroepitaxially grown on top of substrates from different materials (Fig5).

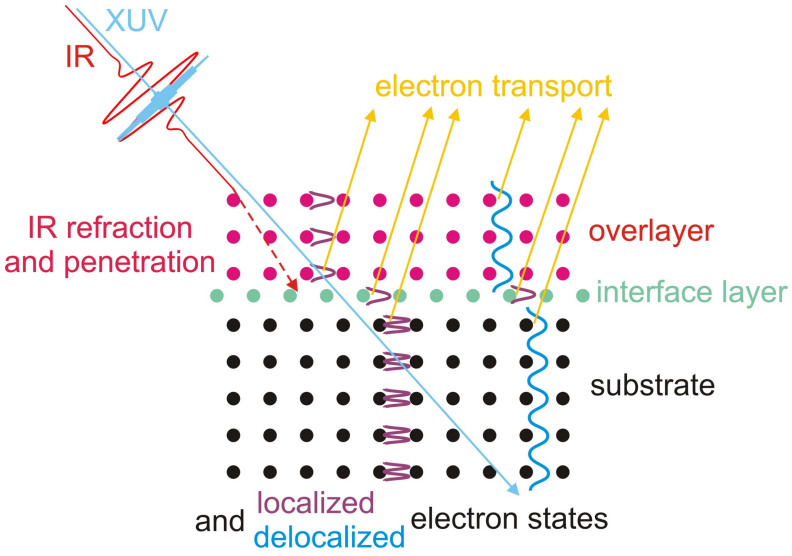

Fig.5 : For a better understanding of the streaking process it is necessary to discriminate the influences of electron localization; electron transport; surface and interface barriers; and refraction and penetration

of the IR streaking field. Appropriately tailored crystalline sandwich structures of different materials, metallic and insulating, can help to solve this task (from [16]).

By varying thickness and elemental composition of these layered samples, transport and electronic properties could by varied independently and disentangled. Experiments with different photon energies will test the influence of final state effects and give insight into this problem.

Acknowledgements

Support by the Deutsche Forschungsgemeinschaft through the Excellence Cluster Munich Centre for Advanced Photonics, Research Area A1 and C1 is acknowledged. RK acknowledges support from an ERC Starting Grant.

References

[1] M. Hentschel et al., Nature 2001, 414, 501.
[2] E. Goulielmakis et al. Science 2004, 305, 1267.
[3] A. Baltuska et al., Attosecond control of electronic processes by intense light fields, Nature 2003, 421, 611.
[4] R. Kienberger et al. Science 2002, 297, 1144.
[5] Kienberger R., Goulielmakis E., Uiberacker M., Baltuska A., Yakovlev V., Bammer F., Scrinzi A., Westerwalbesloh Th., Kleineberg U., Heinzmann U., Drescher M. & Krausz F. Atomic transient recorder. *Nature* **427,** 817-821 (2004).
[6] A. Cavalieri et al., Nature 2007, 449, 1029.
[7] Kienberger R, Krausz F: Single sub-fs XUV pulses: generation and measurement, Proceedings of the Society of Photo-Opitcal Instrumentation Engineers (SPIE), **5580,** 644-658 (2005)
[8]. Brabec, T. & Krausz, F. Intense few-cycle laser fields: frontiers of nonlinear optics. *Rev. Mod. Phys.* **72,** 545-591 (2000).
[9] Goulielmakis E., Schultze M., Hofstetter M., Yakovlev V., Gagnon J., Uiberacker M., Aquila A.L., Gullikson A.M., Attwood D.T., Kienberger R., Krausz F., Kleineberg U.: "Single-cycle nonlinear optics", Science **320**, 1614 (2008).
[10] Wheatstone, C. *Phil. Mag.* **6,** 61 (1835).
[11] Bradley, D. J., Liddy, B., & Sleat, W. E., *Opt. Commun.* **2,** 391 (1971).

[12] Schelev, M. Ya, Richardson, M. C., & Alcock, A. J., Image-converter streak camera with picosecond resolution. *Appl. Phys. Lett.* **18,** 354 (1971).
[13] Itatani, J., Quéré, F., Yudin, G. L., Ivanov, M. Yu, Krausz, F., & Corkum, P. B. Attosecond streak camera. *Phys. Rev. Lett.* **88,** 173903 (2002).
[14] Kitzler, M., Milosevic, N., Scrinzi, A., Krausz, F., & Brabec, T. Quantum theory of attosecond XUV pulse measurement by laser-dressed photoionization. *Phys. Rev. Lett.* **88**, 173904 (2002).
[15] Kane, D. J. & Trebino, R. Characterization of arbitrary femtosecond pulses using frequency-resolved optical gating. *IEEE J. Quantum Electron.* **29,** 571-579 (1993).
[16] Sekikawa, T., Katsura, T., Miura, S., & Watanabe, S. Measurement of the intensity-dependent atomic dipole phase of a high harmonic by frequency-resolved optical gating. *Phys. Rev. Lett.* **88,** 193902 (2002).
[17] A.Cavalieri, F. Krausz, R. Ernstorfer, R. Kienberger, P. Feulner, J. Barth, D. Menzel: „Attosecond Time-Resolved Spectroscopy at Surfaces“ (invited), in „Dynamics at Solid Surfaces and Interfaces“, Wiley-VCH (2010).
[18] A. K. Kazansky and P.M. Echenique, Phys. Rev. Lett. 102, 177401 (2009).
[19] C.-H. Zhang and U. Thumm, Phys. Rev. Lett. 102, 123601 (2009).
[20] C. Lemell, B. Solleder, K. Tökési and J. Burgdörfer, Phys. Rev. A79, 062901 (2009)